Materials Science and Engineering B 111 (2004) 25–30

MATERIALS SCIENCE & ENGINEERING B

www.elsevier.com/locate/mseb

Ferroelectric lead magnesium niobate–lead titanate single crystals for ultrasonic hydrophone applications

S.T. Lau [a,*], K.H. Lam [a], H.L.W. Chan [a], C.L. Choy [a], H.S. Luo [b], Q.R. Yin [b], Z.W. Yin [b]

[a] Department of Applied Physics and Materials Research Centre, The Hong Kong Polytechnic University, Hunghom, Kowloon, Hong Kong, China
[b] Shanghai Institute of Ceramics, The Chinese Academy of Sciences, Shanghai, China

Received 19 November 2003; accepted 3 February 2004

Abstract

Ferroelectric lead magnesium niobate–lead titanate (PMN–PT) single crystals with a composition around the rhombohedral–tetragonal morphotropic phase boundary (65 mol% of PMN) were used to fabricate single-element needle-type hydrophones for measuring the spatial and temporal characteristics of medical ultrasonic transducers. PMN–PT single crystal was grown by a modified Bridgman method. Discs (0.5 mm thick) with normal along the $\langle 0\,0\,1\rangle$ direction were cut and then poled by a dc field in the thickness direction. The single crystal has a high relative permittivity ($\varepsilon_r \sim 4000$) making it appropriate for small area hydrophone applications. Single-element needle-type hydrophones with this material as the sensing element have been fabricated and characterized. The hydrophones have flat frequency response and good receiving sensitivity over certain frequency range in the megahertz region.

Keywords: Relaxor ferroelectrics; PMN–PT single crystal; Piezoelectric; Hydrophone

1. Introduction

In the 1950s, lead-based relaxor materials with the chemical form of $Pb(B'B'')O_3$ were first discovered by Smolenskii et al. [1]. The potential piezoelectric properties of perovskite (ABO_3) structure of $Pb(Zr_{1-x}, Ti_x)O_3$ (PZT) ceramics near the morphotropic phase boundary (MPB) separating the rhombohedral and tetragonal phases were first clarified by Jaffe et al. in 1955 [2]. After the discovery of PZT system, numerous $Pb(B'B'')O_3$ and $Pb(B'B'')O_3$–$PbTiO_3$ materials similar to PZT began to attract special attention from researchers. Among these materials, lead magnesium niobate–lead titanate [$x\mathrm{Pb(Mg_{1/3}Nb_{2/3}}-(1-x)\,\mathrm{PbTiO_3}$, abbreviated as PMN–PT] is an important system which has been widely studied in recent years [3–6].

The PMN–PT solid solution system exhibits ultrahigh relative permittivity ($\varepsilon_r = 3500$–5000 at 1 kHz) and piezoelectric properties ($d_{33} = 1500$–3000 pC/N, $k_{33} > 0.9$ and $k_t \sim 0.6$) [7]. These excellent properties are found in PMN–PT single crystals with compositions near the MPB region (at ∼65 mol% PMN) [4,7]. At this composition, the coexistence of possible crystal structures produces inhomogeneity in the structure of this solid solution system by combing the rhombohedral PMN and the tetragonal PT. The enhanced polarizability arising from the coupling between these two equivalent energy states may explain the origin for the outstanding properties observed in PMN–PT systems.

In recent years, the demand for quantitative assessments of both spatial and temporal characteristics of medical ultrasonic fields in the megahertz frequency range has grown rapidly. Piezoelectric polymers such as polyvinylidene fluoride (PVDF) and vinylidene fluoride–trifluoroethylene [P(VDF–TrFE)] have been used as active elements in hydrophones [8–11], and various commercial devices of this type are available. However, they exhibit low sensitivities and the low relative permittivity of polymer hydrophones are not desirable because the output signals of the sensing elements are greatly reduced by the capacitance of the coaxial cables. These shortcomings limit their receiving sensitivity when used for acoustic field characterization at high frequency. Therefore, due to their outstanding electrical properties, PMN–PT single crystals can be promising materials for high-frequency medical sensors and transducers [12,13].

In the present work, we aim to use PMN–PT single crystals as the sensing elements to fabricate needle-type hy-

* Corresponding author. Tel.: +852-27664098; fax: +852-23337629.
E-mail address: ap-s.t.lau@polyu.edu.hk (S.T. Lau).

0921-5107/$ – see front matter © 2004 Elsevier B.V. All rights reserved.
doi:10.1016/j.mseb.2004.02.016

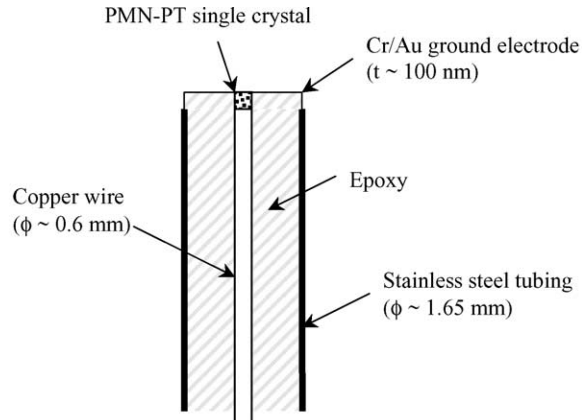

(a)

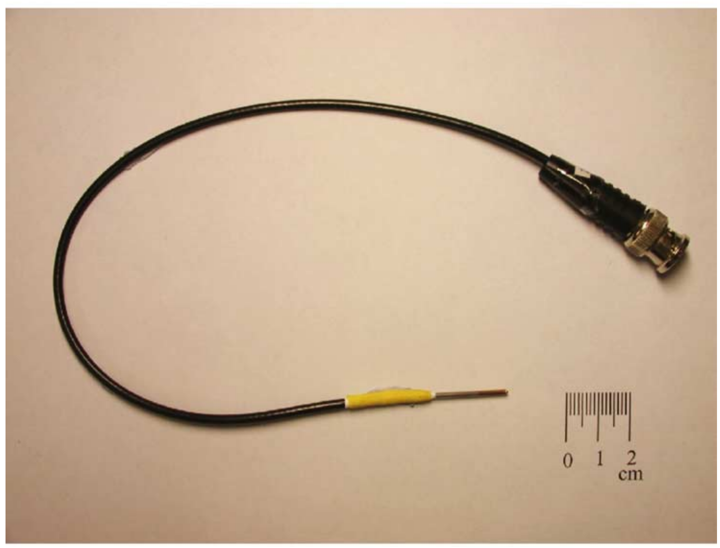

(b)

Fig. 1. (a) Schematic diagram of a needle-type hydrophone (b) photograph of the needle-type hydrophone.

drophones operating in the megahertz frequency range. The permittivity and resonance characteristics of PMN–PT single crystals are measured. The performances of these newly developed hydrophones are evaluated.

2. Material used

PMN–PT single crystal with 65 mol% of PMN was grown by a modified Bridgman method [14]. Chromium–gold (Cr/Au) layers of thickness ∼100 nm were sputtered on both sides of the sample surfaces as electrodes. The 0.5 mm thick PMN–PT single crystal was cut into several small elements (∼ 1 mm × 1 mm and ∼0.5 mm × 0.5 mm) with normal along the ⟨0 0 1⟩ direction. To induce the piezoelectric properties, the PMN–PT discs were poled under a dc field of 1 MV/m at 140 °C for 10 min in the thickness direction. The poled samples were short-circuit at 50 °C for 24 h in order to remove the trapped charges.

3. Characterization of the PMN–PT single crystal

The capacitance C of the PMN–PT disc was measured by an impedance/gain phase analyzer (Hewlett–Packard 4194A). The relative permittivity (ε_r) of the sample can be determined using the following equation:

$$\varepsilon_r = \frac{Ct}{\varepsilon_0 A} \qquad (1)$$

where ε_0 is the permittivity of free space ($=8.85 \times 10^{-12}$ F/m), A the area of the electroded surface of the disc and t is the thickness of the disc.

Table 1
Physical characteristics of the PMN–PT sensing elements

Sample hydrophone	Width (mm)	Length (mm)	Thickness (mm)
N1	0.9	0.9	0.5
N2	0.5	0.48	0.5
N3	0.5	0.45	0.25

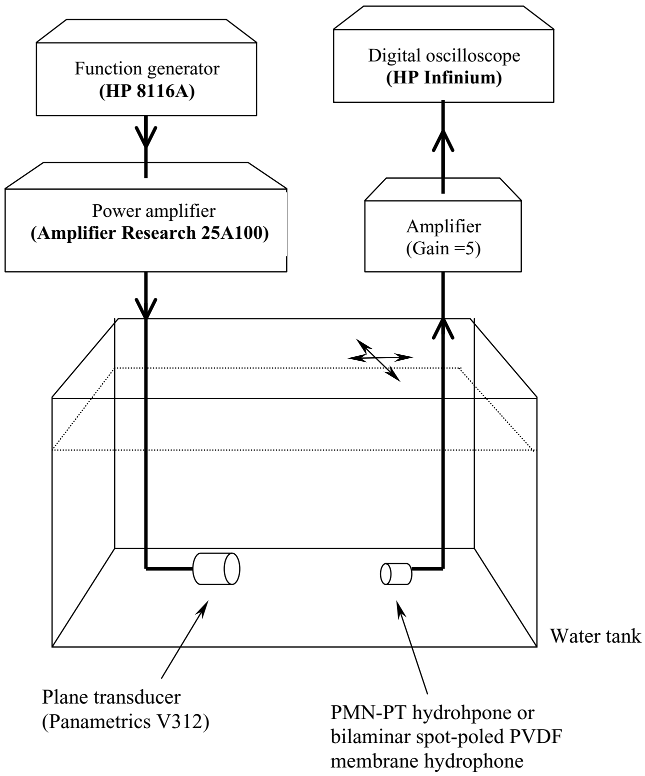

Fig. 2. Experimental setup for testing the sensitivity of the hydrophones.

As the vibration characteristics of the single crystal can be excited electrically, the HP4194A impedance analyzer was also used to measure the electrical impedance of the sample as a function of frequency in order to determine its resonance frequencies. The electromechanical coupling factor (k_t) and frequency constant (N_t^{D}) in the thickness direction can be calculated from the resonance and anti-resonance frequencies (f_{r} and f_{a}) according to the IEEE standard on piezoelectricity [15]:

$$k_t = \sqrt{\frac{\pi}{2}\frac{f_{\mathrm{r}}}{f_{\mathrm{a}}}\tan\left(\frac{\pi}{2}\frac{f_{\mathrm{a}}-f_{\mathrm{r}}}{f_{\mathrm{a}}}\right)} \tag{2}$$

$$N_t^{\mathrm{D}} = f_{\mathrm{r}} \times t \tag{3}$$

Using the equivalent circuit analysis built in to the HP4194A impedance analyzer, the effective mechanical (Q_{m}) factor of the single crystal can be estimated by:

$$Q_{\mathrm{m}} = \frac{\omega L}{R} \tag{4}$$

where ω is the angular frequency and L and R are the inductance and resistance deduced from the equivalent circuit of a piezoelectric vibrator [15]. The piezoelectric charge coefficient (d_{33}) was measured using a d_{33} meter (ZJ-3B) supplied by the Beijing Institute of Acoustics, Academia Sinica.

4. Construction and evaluation of the hydrophones

After characterizing the electromechanical properties of the PMN–PT single crystals, the crystals were then cut into small tiles and used as the sensing element for fabricating the needle-type hydrophones. The structure of the needle hydrophone is shown schematically in Fig. 1a. A copper wire with a diameter of 0.6 mm was placed in the center of a stainless-steel tubing with a diameter of 1.65 mm. Epoxy (Ciba–Geigy, 5 min Araldite) was used to hold the copper wire in the center of the tubing. To expose the tip of the wire, the tip of the needle head was polished using a 1000 mesh (25 μm) emery paper. The PMN–PT single crystal was glued to the tip of the exposed wire using silver paint (Agar Scientific Ltd.) and the edge of the crystal was then covered by epoxy. A Cr/Au electrode was sputtered on the surface of the sensing element to make contact with the tubing and

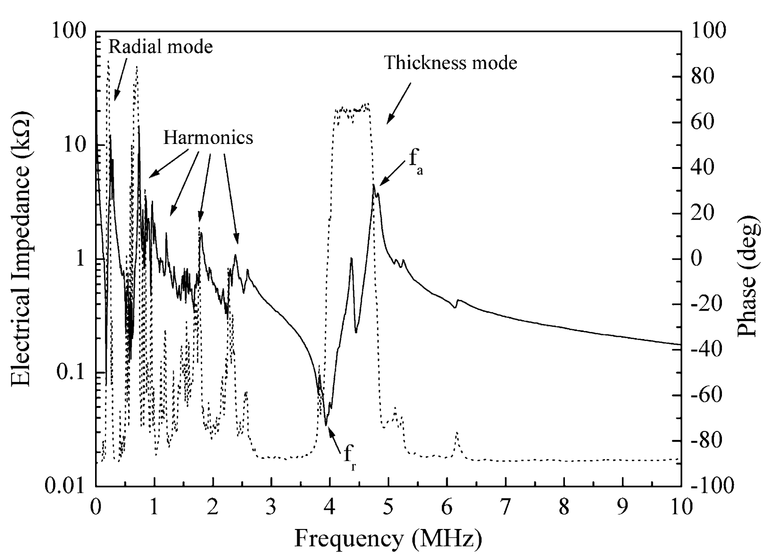

Fig. 3. The impedance (solid line) and phase (dotted line) vs. frequency spectra of a PMN–PT single crystal.

acted as the ground electrode. Finally, the needle-head was connected to a 50 Ω coaxial cable for transmitting the signal to an amplifier (Fig. 1b). As the hydrophone was used under water, the connection between the needle-head and the coaxial cable was covered by silicone rubber to prevent ingression of water. In the present study, three needle-type hydrophones have been fabricated with single crystal of different sizes and the detail descriptions are listed in Table 1.

Testing of the hydrophones was carried out in a water tank (Fig. 2). The receiving sensitivity of the sample hydrophone is determined by a comparison method in which the received signal from the sample hydrophone is compared with that of a reference hydrophone with known sensitivity. A transducer with diameter of 6.35 mm (Panametrics V312) was used to produce the acoustic waves. The sample hydrophone was placed at a point within the far field region of the transducer (*distance* $> a^2/\lambda$, where a is the transducer radius and λ is the wavelength of the acoustic wave). The hydrophone was positioned for maximum signal in the plane perpendicular to the transducer axis and measurements were made with the transducer excited by a 20-cycle tone burst with driving voltage in the frequency range of 1–24 MHz. The hydrophone output signal was measured over the region of the tone burst for which a voltage waveform of constant amplitude was observed using an oscilloscope (HP Infinum). For comparison, the sample hydrophone was replaced by a standard bilaminar PVDF membrane hydrophone (Type Y-34-3598 GCE-Marconi) at the same position and the signal of the membrane hydrophone was measured using the same procedure. The sensitivity M_a at the output of the amplifier connected to the PMN–PT hydrophone is calculated from:

$$M_a = \left(\frac{V_L}{V_S}\right) M_S \qquad (5)$$

where V_L and V_S are the voltage measured by the PMN–PT and membrane hydrophones, respectively, and M_S is the end-of-cable loaded sensitivity of the membrane hydrophone (with the amplifier). The end-of-cable loaded sensitivity of PMN–PT hydrophone M_L is then given by:

$$M_L = \frac{M_a}{G} \qquad (6)$$

where G is the gain of the amplifier ($G = 5$).

5. Results and discussion

5.1. Characterization of the PMN–PT single crystal

The performance of PMN–PT single crystal was evaluated by the impedance analyzer and piezoelectric d_{33} meter. To understand the vibration characteristics of the single crystal, its electric impedance and phase are measured as a function of frequency and the results are given in Fig. 3. In the impedance spectrum, many resonance and anti-resonance peaks are observed which are contributed by two main vibrational modes (the radial and thickness modes) and several harmonics. As shown in Fig. 3, unlike lead zirconate titanate (PZT) ceramics, the harmonics of the radial mode in PMN–PT single crystals are quite scattered presumably due to anisotropy in the planar directions. The resonance fre-

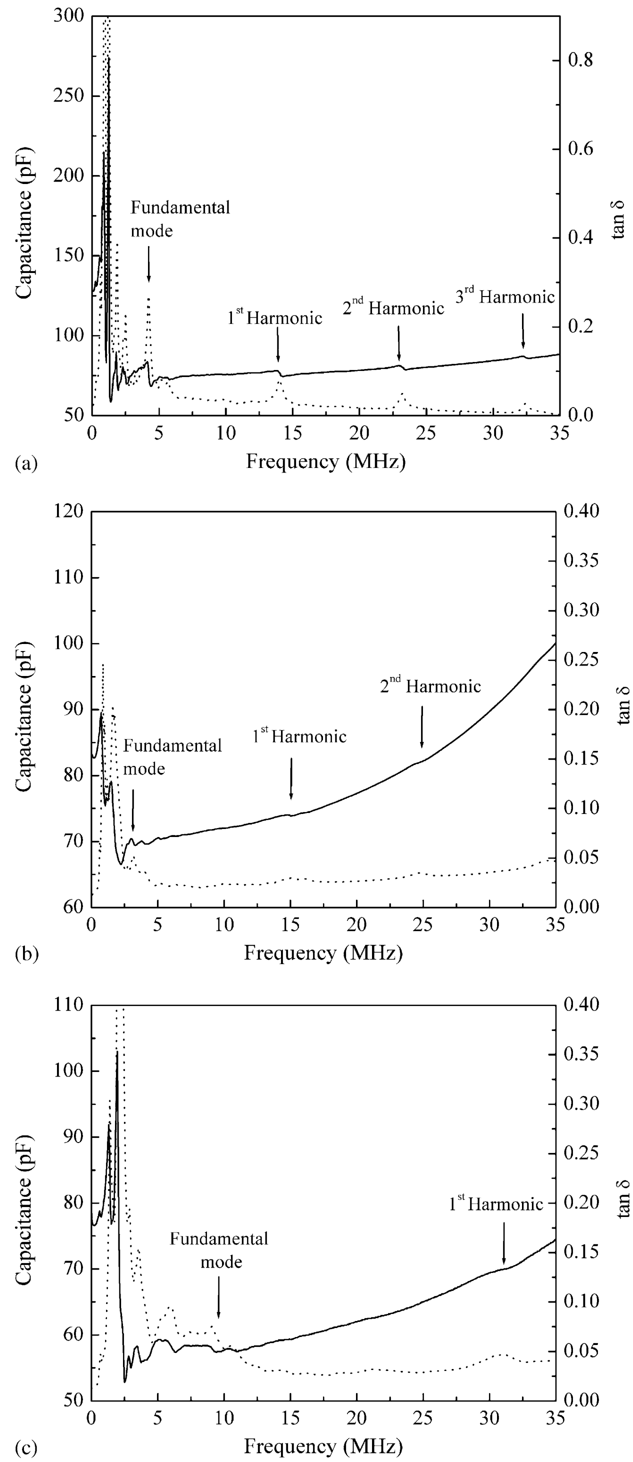

Fig. 4. The capacitance (solid line) and tan δ (dotted line) vs. frequency spectra of the PMN–PT hydrophones: (a) N1, (b) N2 and (c) N3.

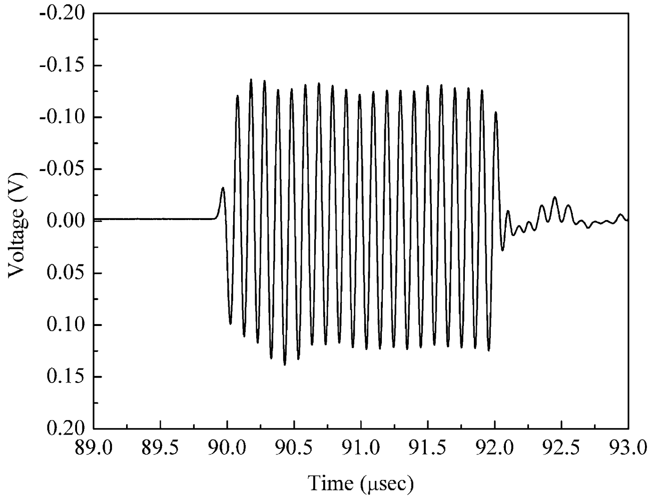

Fig. 5. The waveform of the voltage signal received by the PMN–PT hydrophone N1.

quencies f_r and f_a of the thickness mode vibration are found at 3.91 and 4.75 MHz. With the measured frequencies, the values of k_t and N_t^D of the PMN–PT disc were found to be 0.61 and 1916 Hz-m by using Eqs. (2) and (3), respectively. The capacitance of the single crystal was measured and the relative permittivity ε_r at 1 kHz was found to be 4000. The effective mechanical quality factor Q_m of the single crystal was found to be ∼60. The piezoelectric coefficient d_{33} of PMN–PT crystal was 1500 pC/N.

5.2. Performance of PMN–PT needle-type hydrophones

The end-of-cable capacitance of the three needle-type hydrophones was measured in the frequency range of 1–35 MHz using the HP 4194A impedance analyzer and the capacitance spectra are presented in Fig. 4 where several resonance and anti-resonance peaks are observed. For hydrophones N1 and N2 (Fig. 4a and b), the thickness mode vibration appears at about 4 MHz which is closed to that observed in the free-standing single crystal. For hydrophone N3 (Fig. 4c), the thickness of the sensing element has been reduced to half of those in hydrophones N1 and N2, and its thickness mode resonance shifts to higher frequency. Besides, the frequency of fundamental thickness mode and its harmonics are further separated. A hydrophone normally operates in the frequency range away from the resonances in order to obtain a flat frequency response. Therefore, by increasing the separation between the resonance frequencies, we can design a hydrophone with wideband response to the acoustic field.

The waveforms of the voltage signal received by the PMN–PT hydrophones N1 to a tone burst at 10 MHz is shown in Fig. 5. Similar waveforms are observed in other hydrophones. It can be seen that no distortion is observed in the waveform. The end-of-cable loaded sensitivities of the hydrophones were measured by the comparison method.

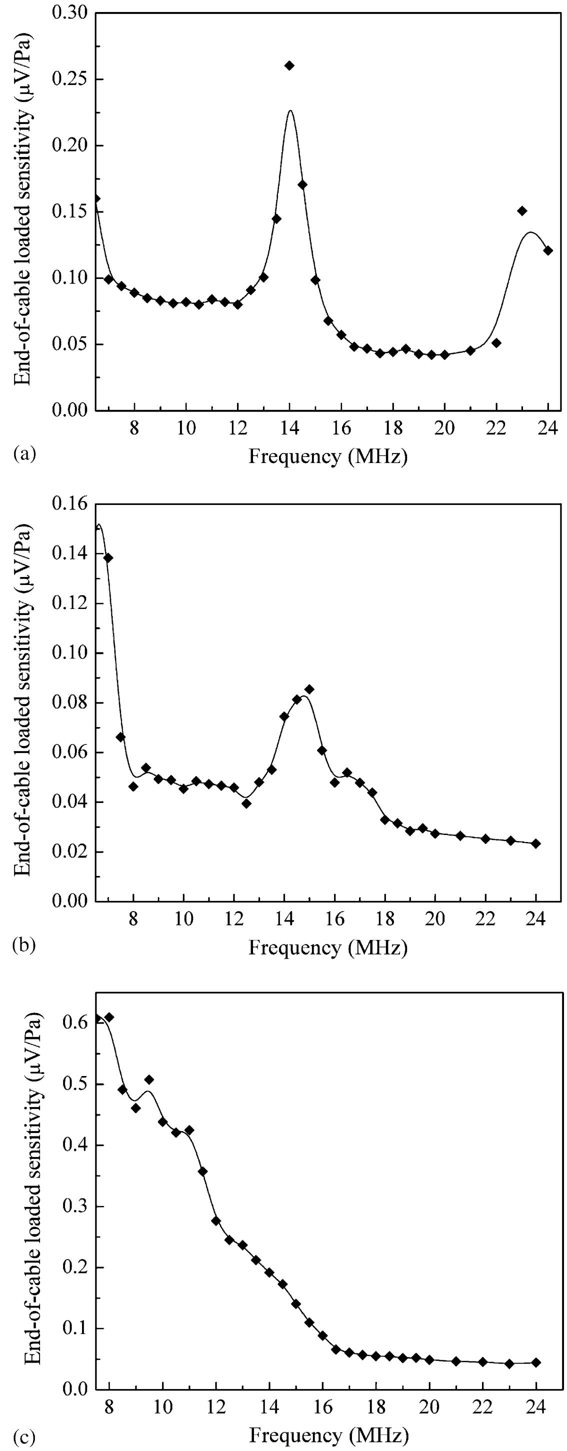

Fig. 6. Frequency plot of the end-of-cable loaded sensitivity M_L for the PMN–PT hydrophones: (a) N1, (b) N2 and (c) N3.

Fig. 6 presents the frequency plots of the sensitivity for the three PMN–PT hydrophones. In Fig. 6a, the hydrophone N1 shows a flat sensitivity in the frequency ranges of 7–12 and 17–22 MHz. The peaks at 14 and 23 MHz correspond to the resonances in the PMN–PT single crystals. For hydrophone N2 (Fig. 6b), the diameter of the sensing ele-

Table 2
Comparison between the hydrophones fabricated using PVDF and PMN–PT single crystals

Hydrophone type	Sensing area (mm^2)	Thickness (μm)	End-of-cable loaded sensitivity M_L (μV/Pa)
PMN–PT needle-like (N1)	0.81	500	0.082 at 10 MHz
PMN–PT needle-like (N2)	0.24	500	0.045 at 10 MHz
PMN–PT needle-like (N3)	0.23	250	0.049 at 20 MHz
PVDF membrane [16]	0.20	25	0.040 at 1 MHz 0.031 at 20 MHz

ment is reduced by half in comparison with that of hydrophone N1, both sensitivity and the resonance peak amplitude decrease. Since thickness of the active elements in both N1 and N2 is the same, the resonances occur at similar frequencies. Therefore, to obtain a flat frequency response in a wider frequency range, the resonance peak should be shifted to higher frequency by thinning down the active element. As shown in Fig. 6c, the hydrophone N3 shows a flat sensitivity in the frequency ranged from 17 to 24 MHz. Table 2 lists the M_L values for a PVDF membrane hydrophone and PMN–PT single crystal hydrophones. The M_L values of membrane-type PVDF hydrophone with similar sensing element size (area ∼0.2 mm^2) are ∼0.04 μV/Pa at 1 MHz and 0.031 μV/Pa at 20 MHz. All the PMN–PT hydrophones have higher M_L. Even for N3, the M_L value is ∼0.05 μV/Pa at 20 MHz which is nearly 25% higher than that of the PVDF hydrophone. Therefore, this newly developed PMN–PT hydrophone can operate at high frequency (in the range of 17–24 MHz) with good receiving sensitivity.

6. Conclusion

PMN–PT single crystals with 65 mol% of PMN, grown by the modified Bridgman method, have been characterized. The single crystal has good electromechanical properties, with high value of piezoelectric coefficient (d_{33} ∼1500 pC/N). Besides, it has high relative permittivity (ε_r ∼4000 at 1 kHz), which is an advantage in alleviating the cable shunting problem. The single crystals were used as the sensing elements of several needle-type hydrophones. The performance of the hydrophones was evaluated in water. By thinning the single crystal to proper dimensions, the resonances of the crystal can be shifted to higher frequencies and the PMN–PT hydrophone shows flat frequency response ranged from 17 to 24 MHz. In comparison with typical PVDF hydrophones, the PMN–PT hydrophones have higher receiving sensitivity.

Acknowledgements

This work was supported by the Centre for Smart Materials of The Hong Kong Polytechnic University and partially supported by a grant from the Research Grants Council of The Hong Kong Special Administrative Region (Project No.: PolyU 5193/00P).

References

[1] G.A. Smolenskii, A.I. Agranovskaya, Sov. Phys. Tech. Phys. 3 (1958) 1380.
[2] B. Jaffe, R.S. Roth, S. Marzullo, J. Res. Natl. Bur. Standard 55 (1955) 239.
[3] J. Kuwata, K. Uchino, S. Nomura, Jpn. J. Appl. Phys. 21 (1982) 1298.
[4] S.W. Choi, T.R. Shrout, S.J. Jang, A.S. Bhalla, Ferroelectrics 100 (1989) 29.
[5] R.F. Service, Science 275 (1997) 1878.
[6] H. Fu, R.E. Cohen, Nature 403 (2000) 281–283.
[7] H. Luo, G. Xu, H. Xu, P. Wang, Z. Yin, Jpn. J. Appl. Phys. 39 (2000) 5581.
[8] M. Platte, Ultrasonics 23 (1985) 113.
[9] H.L.W. Chan, A.H. Ramelan, I.L. Guy, D.C. Price, Rev. Sci. Instrum. 62 (1991) 203.
[10] K. Koyama, T. Eda, H. Suzuki, Y. Wada, O. Ishizuka, Acoust. Imaging 17 (1989) 579.
[11] P.A. Lewin, R. Bautista, V. Devaraju, Ultrasound Med. Biol. 25 (1999) 1131.
[12] J. Chen, A. Shurland, J. Perry, B. Ossmann, T.R. Gururaja, in: Proceedings of the 10th IEEE International Symposium on Applications of Ferroelectrics, East Brunswick, NJ, USA, 18–21 August 1996, pp. 27–30.
[13] Q.R. Yin, J.W. Fang, H.S. Luo, G.R. Li, in: Proceedings of the 12th IEEE International Symposium on Applications of Ferroelectrics, Honolulu, Hawaii, USA, 21 July–2 August 2000, pp. 569–572.
[14] Z.W. Yin, H.S. Luo, P.C. Wang, G.S. Xu, Ferroelectrics 229 (1999) 207–216.
[15] An American National Standard, IEEE Standard on Piezoelectricity (Std 176), The Institute of Electrical and Electronics Engineers Inc., USA, 1987.
[16] Certificate of Calibration, PVDF Ultrasonic Hydrophone Type Y-34-3598, National Physical Laboratory, 1993.